5th Canadian Conf. Earthquake Engineering / Ottawa / 1987 / 5ème Conf. Canadienne Génie Sismique

Ultimate shear strength of RC beams with high tension shear reinforcement and high strength concrete

Katsumi Kobayashi
Fukui University, Japan
Seiji Kokusho
Tokyo Institute of Technology, Yokohama, Japan
Yasuhiro Matsuzaki
Tokyo Science University, Japan
Tetsumitsu Eigawa
Neturen Co. Ltd, Tokyo, Japan

ABSTRACT: In the experiment of reinforced concrete beams with high tension shear reinforcement, it was proved that the ultimate shear strength was increased by using high strength concrere in all the range of $Pw \cdot w\sigma y$. Here Pw is the shear reinforcement ratio and $w\sigma y$ is its yield strength. It was also proved that the relation between the ultimate shear strength and $Pw \cdot w\sigma y$ can be divided into two parts and that the range of $Pw \cdot w\sigma y$, where the full strength of shear reinforcement was showed at shear failure, expanded according to the increase of the strength of concrete. The experimental results were well followed in tendency by the proposed truss model taking account of the compatibility of deformation as well as the equilibrium of forces.

1 INTRODUCTION

In this study, the high tension steel bar "ULBON" is used as shear reinforcement of reinforced concrete beams. ULBON with yield strength over 13000 kg/cm^2 is generally used as prestressing steel for prestressed concrete members and has three or six helical grooves on its surface for good bond with concrete. It had been applied to reinforced concrete structures as a shear reinforcement just a few years ago. And some experimental works were made (Fukuhara, 1979, 1982, 1984), (Muguruma, 1979, 1980, 1981).

This high tension steel can be shaped spirally in round, rectangular or square by cold work according to the design requirement as shown in Fig.1 and Fig.2. In design, the permissible tensile stress under temporary loading 6000 kg/cm^2 and the upper limit of shear reinforcement ratio 0.6 % have been officially approved taking account of the aseismic safety (NETUREN Co., Ltd., 1985) and ULBON is widely used in high-rise reinforced concrete buildings. Over 2000 tons had been used in eleven to twenty-five stories buildings last year. The effectiveness of the high tension shear reinforcement has been highly evaluated (Kobayashi, 1983), (Muguruma, 1985), (Yamaguchi, 1985), (Kokusho, 1986), (ito, 1986) and this study aims the request to develop the design procedure where the high tensile strength can be more highly utilized.

Fig.1 Manufacturing of ULBON spiral

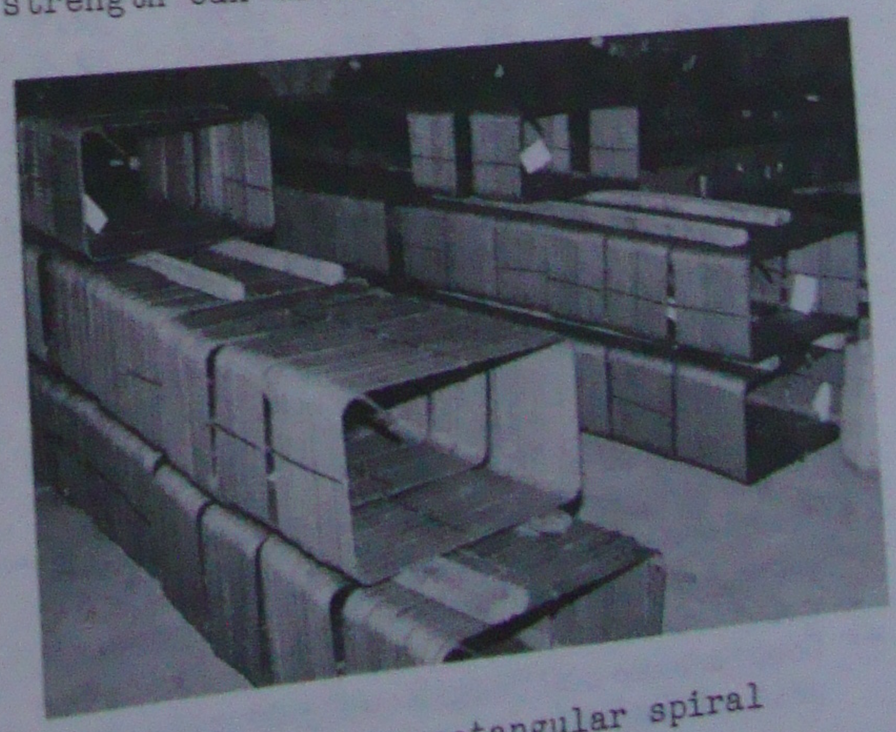

Fig.2 Products of rectangular spiral

In the AIJ Standard for Structural Calculation of Reinforced Concrete Structures, the upper limit of shear reinforcement ratio (Pw) for ordinary strength steel bar is also set up to be 1.2 %. That may be based on the fact that there was few data about shear reinforcing effect over 1.2 % of Pw and that the increase of the ultimate shear strength could not be expected according to the increase of Pw over 1.2 %. In the past study using the high tension shear reinforcement (Fukuhara, 1982), the increase of the ultimate shear strength is also not observed in the range of the large amount of shear reinforcement. These phenomena may be due to the fact that the shear compression failure of concrete goes ahead before the shear reinforcement displays its full strength. Therefore, it is considered that the large tensile strength of the high tension shear reinforcement would be highly utilized, if the shear compression failure could be delayed by using high strength concrete.

The objective of this study is to prove that the ultimate shear strength will increase according to the increase of the strength of concrete and that the range of $Pw \cdot w\sigma y$, where the full strength of the shear reinforcement is displayed at shear failure, will expand with the increase of concrete strength. Furthermore, the shear transfer mechanism is discussed by the simple truss model.

Table 1. Properties of test specimens

No.	Specimen's name*	$C\sigma B$**	Pw (%)	$w\sigma y$ (kg/cm^2)	$Pw \cdot w\sigma y$ (kg/cm^2)
1	B-210- 0	208	0.0	0	0.0
2	B-210- 6.0	208	0.314	13600	42.7
3	B-210- 7.4	208	0.444	14500	64.4
4	B-210- 9.2	208	0.711	14300	101.7
5	B-210-11.0	208	1.000	14600	146.0
6	B-360- 0	383	0.0	0	0.0
7	B-360- 4.1	383	0.147	14200	20.9
8	B-360- 5.1	383	0.227	14500	32.9
9	B-360- 6.0	383	0.314	13600	42.7
10	B-360- 7.4	383	0.444	14500	64.4
11	B-360- 9.2	383	0.711	14300	101.7
12	B-360-11.0	383	1.000	14600	146.0
13	B-570- 0	549	0.0	0	0.0
14	B-570- 4.1	549	0.147	14200	20.9
15	B-570- 6.0	549	0.314	13600	42.7
16	B-570- 7.4	549	0.444	14500	64.4
17	B-570- 9.2	549	0.711	14300	101.7
18	B-570-11.0	549	1.000	14600	146.0

* Specimen's name represents the series name and the diameter of shear reinforcement.
** Compressive strength of concrete in unit of kg/cm^2.

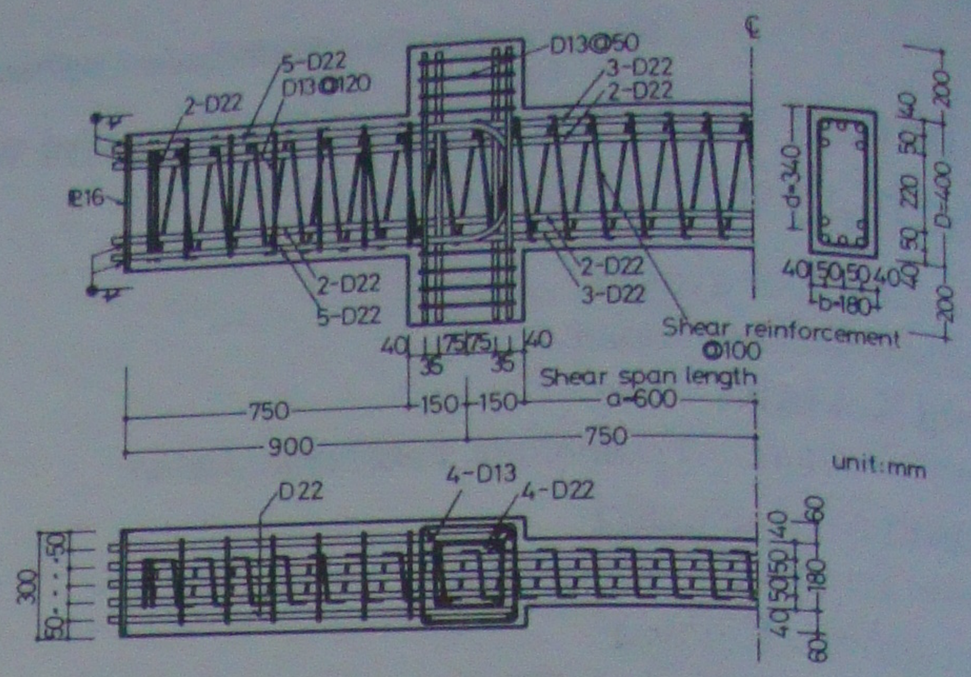

Fig.3 Detail of reinforcing arrangement

2 OUTLINE OF EXPERIMENT

2.1 Specimens

The test specimens are listed in Table 1. The parameters are the diameter of shear reinforcement and the strength of concrete. The size of the specimens and the reinforcing arrangement are shown in Fig.3. The cross section (b x D) is 18 cm x 40 cm and the shear span to depth ratio (a/D) is 1.5 in all specimens. The specimens were longitudinally reinforced by five deformed steel bars of 22 mm nominal diameter both in tensile and compressive side, which yield strength was enhanced up to 8140 kg/cm^2 so as to make shear failure precede. The shear reinforcement was shaped spirally in rectangular with 10 cm intervals. The strength of concrete was initially designed as 210, 360 and 570 kg/cm^2. The actual strength of concrete was shown in Table 2. The mechanical properties of reinforcement are shown in Table 3.

Table 2. Mechanical properties of concrete

Series	$C\sigma B$ (kg/cm^2)	$C\varepsilon B$ ($\times 10^{-6}$)	$cE(1/3)$ ($\times 10^5$ kg/cm^2)	$c\sigma t$* (kg/cm^2)
B-210	208	2315	2.09	20.5
B-360	383	2325	2.59	29.8
B-570	549	2680	2.73	33.2

* Splitting tensile strength

Table 3. Mechanical properties of reinforcing steel bars

Steel bar	$s\sigma_y$* (kg/cm^2)	$s\sigma_{max}$ (kg/cm^2)	sE ($\times 10^6$ kg/cm^2)	Elongation (%)
D22	8140	9130	1.75	10.1
4.1ϕ	14200	15200	2.07	14.1
5.1ϕ	14500	14900	2.04	12.0
6.0ϕ	13600	15000	2.06	10.0
7.4ϕ	14500	15400	2.12	10.2
9.2ϕ	14300	15100	2.12	9.0
11.0ϕ	14600	15400	2.16	10.2

* 0.2% proof stress
Notation $s\sigma y$ is replaced by $w\sigma y$ in case of shear reinforcement.

2.2 Loading and measuring method

Loading apparatus is shown in Fig.4 and illustration of measuring system is shown in Fig.5. The same value of the load (P) was monotonously applied on both of the right and the left stubs and the anti-symmetric bending moment condition was produced.

Gage-holders were set on each stubs. The average of the displacement $\delta 1$ and $\delta 2$, which were measured by the transducers No.1 and No.2, was regarded as the relative displacement. The difference of the rotational displacement of each stub, measured by transducers No.3 through No.6, was hardly observed. Then, the displacement $\delta 1$ and $\delta 2$ were almost same value until reaching the maximum load. The strain of longitudinal reinforcement at the beam end and that of shear reinforcement were measured by strain gages.

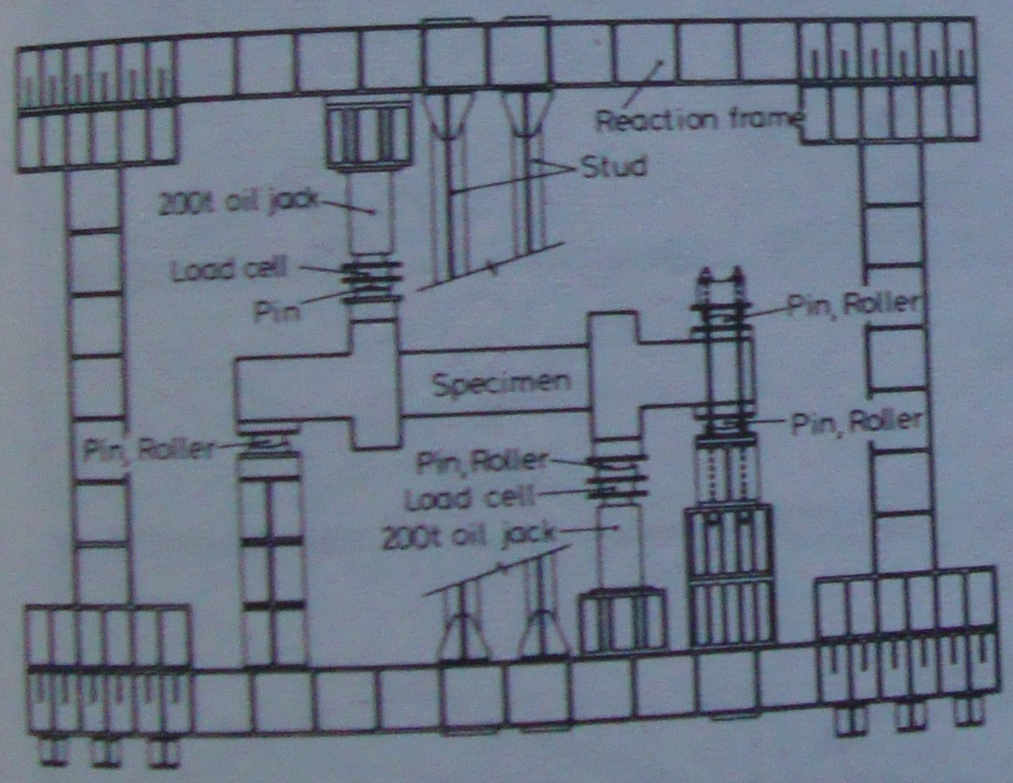

Fig.4 Loading apparatus

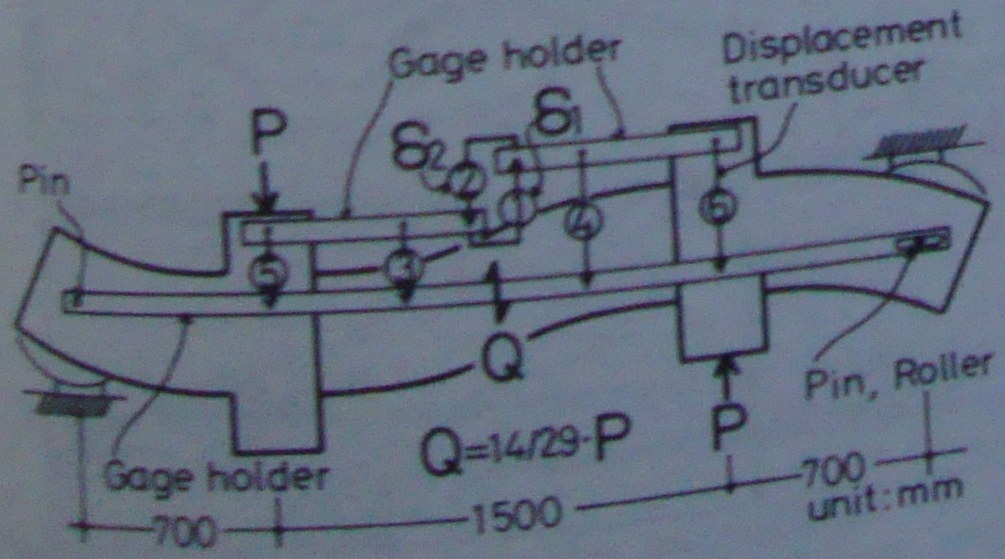

Fig.5 Measuring system

3 EXPERIMENTAL RESULTS

3.1 Relation between shear force and relative displacement

The relations between shear force (Q) and relative displacement (δ) are shown in Fig.6 through Fig.8. As for the specimens without shear reinforcement, the bearing capacity drop quickly when δ is about 5 mm. As for the specimens with shear reinforcement, the ultimate shear force and δ at that time become larger and the restoring force deteriorates rapidly according to the increase of $Pw \cdot w\sigma y$. In the large deflection range, however, the restoring force are almost same regardless of the value of $Pw \cdot w\sigma y$.

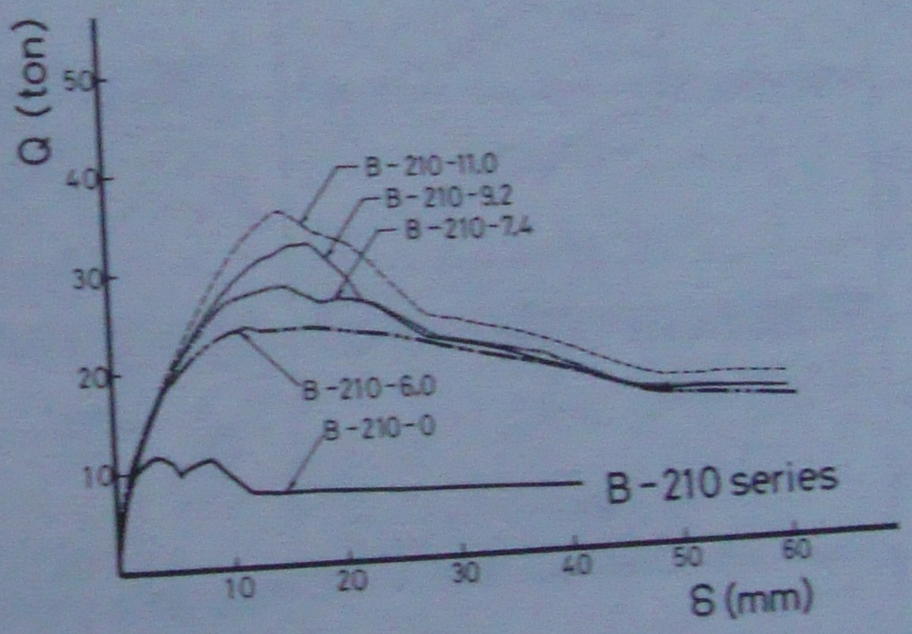

Fig.6 Q - δ curves of B-210 series

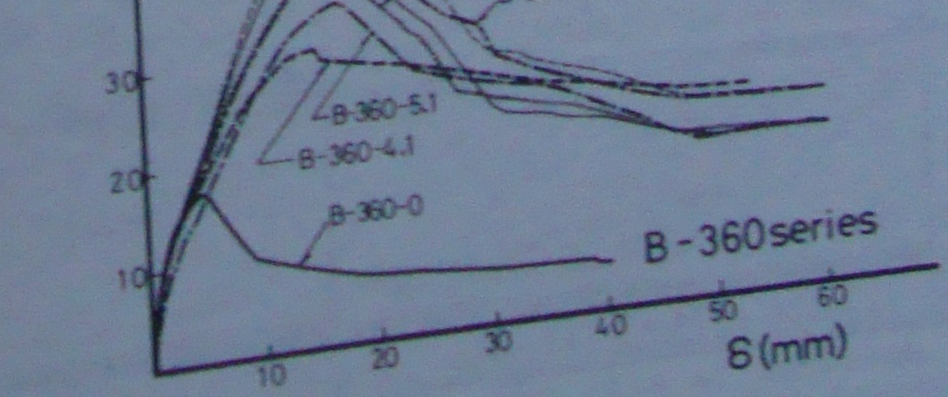

Fig.7 Q - δ curves of B-360 series

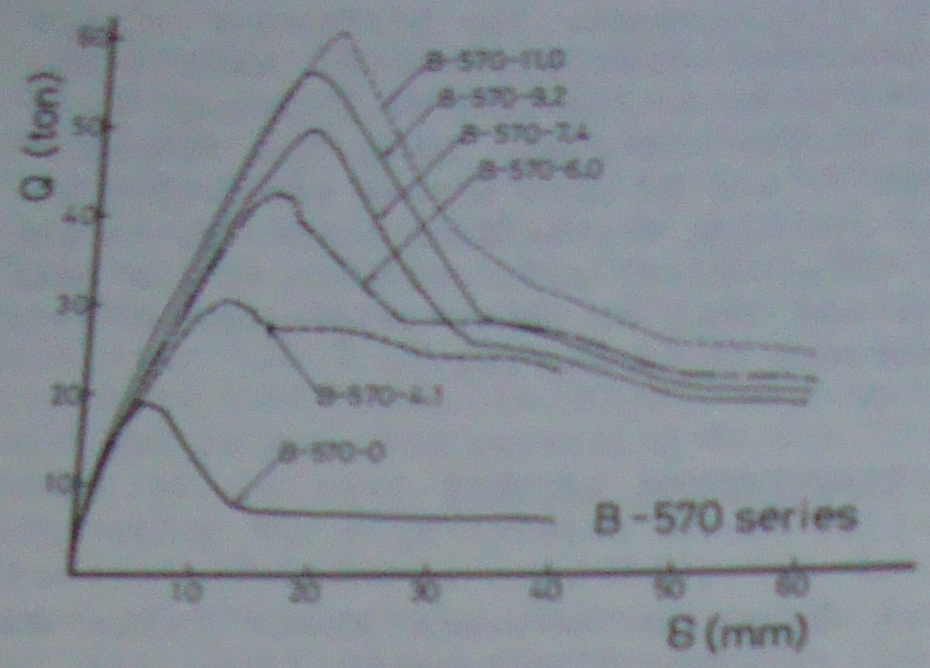

Fig.8 Q - δ curves of B-570 series

3.2 Failure mode

The shear failure occured in all specimens and the yielding of longitudinal reinforcement was not observed. Figure 9 shows the ultimate failure aspect of all specimens. At first, bending shear cracks appear at right and left side of the beam, and then, they develop to splitting cracks along the longitudinal reinforcement. In the range of small $Pw \cdot w\sigma_y$, the splitting cracks come to open and reduce bond resistance. Ultimately the shear reinforcement yields and the shear tension failure occurs as shown in Fig.10. In the range of large $Pw \cdot w\sigma_y$, the opening of the splitting cracks is resisted by the shear reinforcement. Ultimately the diagonal crack appears and the shear compression failure occurs as shown in Fig.11.

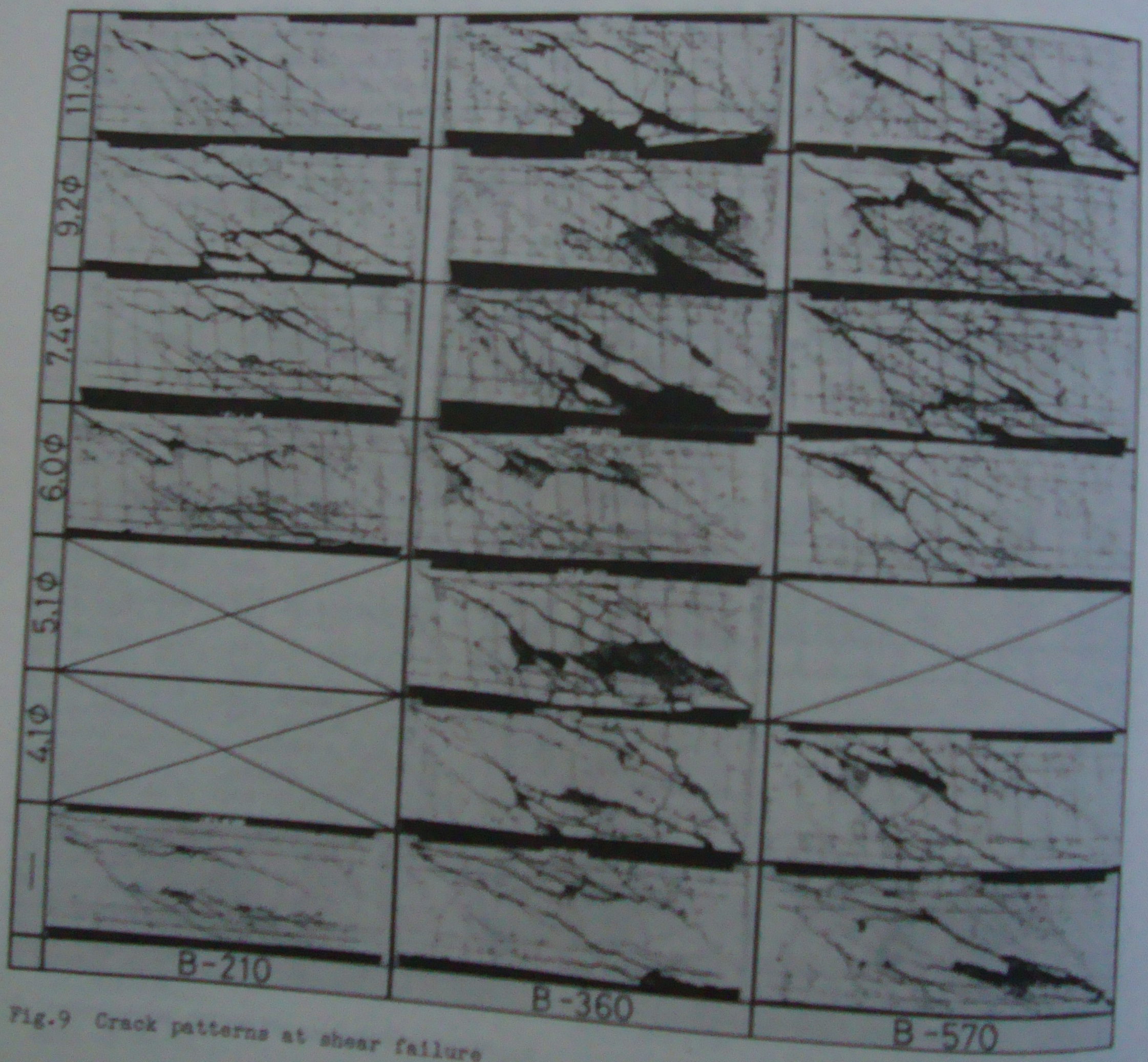

Fig.9 Crack patterns at shear failure

Table 4. Experimental and caluculated value of ultimate shear strength

No.	Specimen's name	$Pw \cdot w\sigma_y$ (kg/cm^2)	Quexp (ton)	τ_{uexp} (kg/cm^2)	$s\tau_{u1}$ (kg/cm^2)	$s\tau_{u2}$ (kg/cm^2)	τ_{My} (kg/cm^2)
1	B-210- 0	0.0	11.6	21.7	18.3	18.3	122.0
2	B-210- 6.0	42.7	24.6	46.0	35.9	53.1	122.0
3	B-210- 7.4	64.4	28.5	53.1	39.9	55.8	122.0
4	B-210- 9.2	101.7	32.8	61.3	45.5	60.4	122.0
5	B-210-11.0	146.0	36.3	67.8	50.9	65.9	122.0
6	B-360- 0	0.0	17.6	32.9	26.5	26.5	127.0
7	B-360- 4.1	20.9	30.8	57.5	38.9	47.4	127.0
8	B-360- 5.1	32.9	35.5	66.3	42.0	59.4	127.0
9	B-360- 6.0	42.7	37.3	69.7	44.2	69.2	127.0
10	B-360- 7.4	64.4	37.5	70.0	48.2	74.1	127.0
11	B-360- 9.2	101.7	46.9	87.6	53.8	78.8	127.0
12	B-360-11.0	146.0	52.0	97.1	59.2	84.3	127.0
13	B-570- 0	0.0	19.4	36.2	34.3	34.3	130.0
14	B-570- 4.1	20.9	30.6	57.1	46.7	55.2	130.0
15	B-570- 6.0	42.7	42.5	79.4	52.0	77.0	130.0
16	B-570- 7.4	64.4	49.5	92.4	56.0	91.6	130.0
17	B-570- 9.2	101.7	56.0	104.6	61.6	96.2	130.0
18	B-570-11.0	146.0	60.5	113.0	66.7	101.7	130.0

Quexp : Maximum shear force in experiment
τ_{uexp} : Average shear stress at maximum shear force in experiment
$s\tau_{u1}$: Ultimate shear strength by Arakawa's τ_{umean} formula
$s\tau_{u2}$: Ultimate shear strength by Fukuhara's formula

$s\tau_{u2} = \mathrm{Min}(st\tau_u , sc\tau_u)$

$st\tau_u = 0.12 \cdot ku \cdot kp(180+Fc)/(M/Qd+0.12) + \alpha \cdot Pw \cdot w\sigma_y \quad (\alpha = 1)$

$sc\tau_u = 0.124 \cdot Pw \cdot w\sigma_y + 824 \cdot Pc + 0.14 \cdot Fc \sqrt{d/a}$

τ_{My} : Average shear stress at bending yield

Fig.10 Crack pattern (1)

Fig.11 Crack pattern (2)

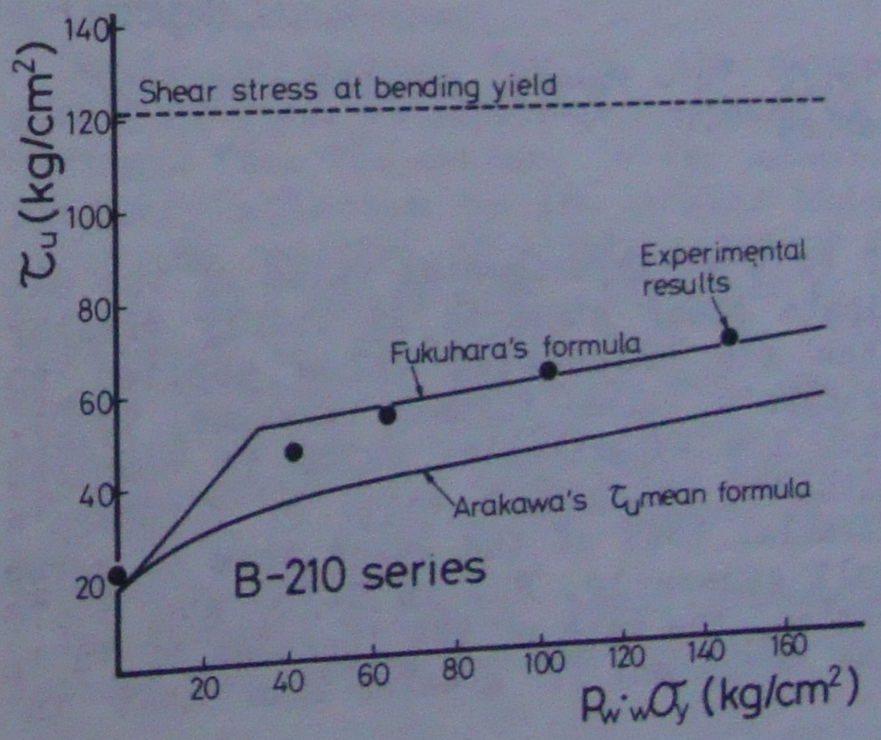

Fig.12 τu - $Pw \cdot w\sigma y$ relations of B-210 series

3.3 Relation between ultimate shear stregth and $Pw \cdot w\sigma y$

The experimental and the calculated value of ultimate shear strength (τu) are shown in Table 4, and the relations between τu and $Pw \cdot w\sigma y$ are shown in Fig.12 through Fig.14. τu increases according to the increase of $Pw \cdot w\sigma y$. The rate of increase of τu is, however, in slow with the increase

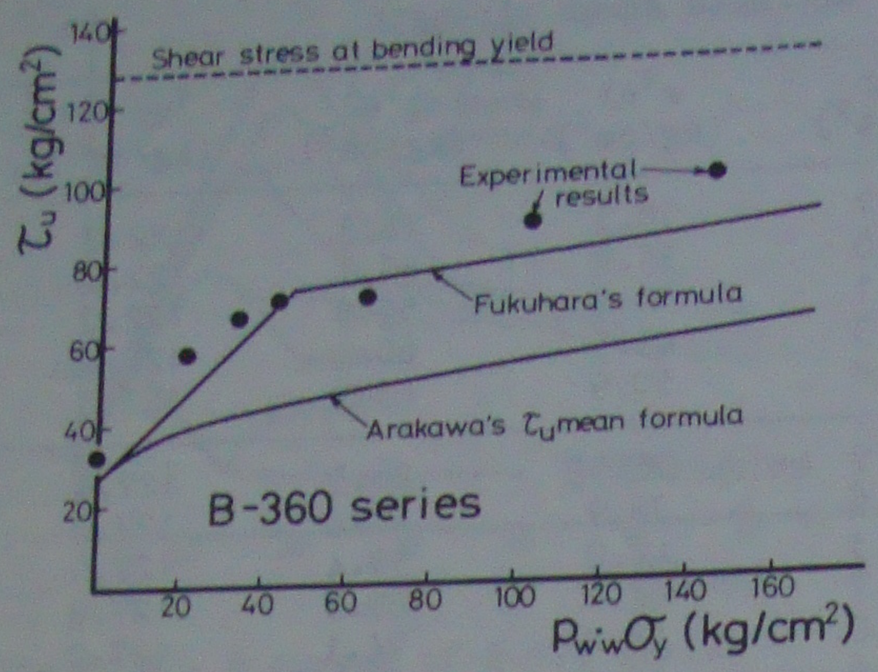

Fig.13 τ_u - $Pw \cdot w\sigma y$ relations of B-360 series

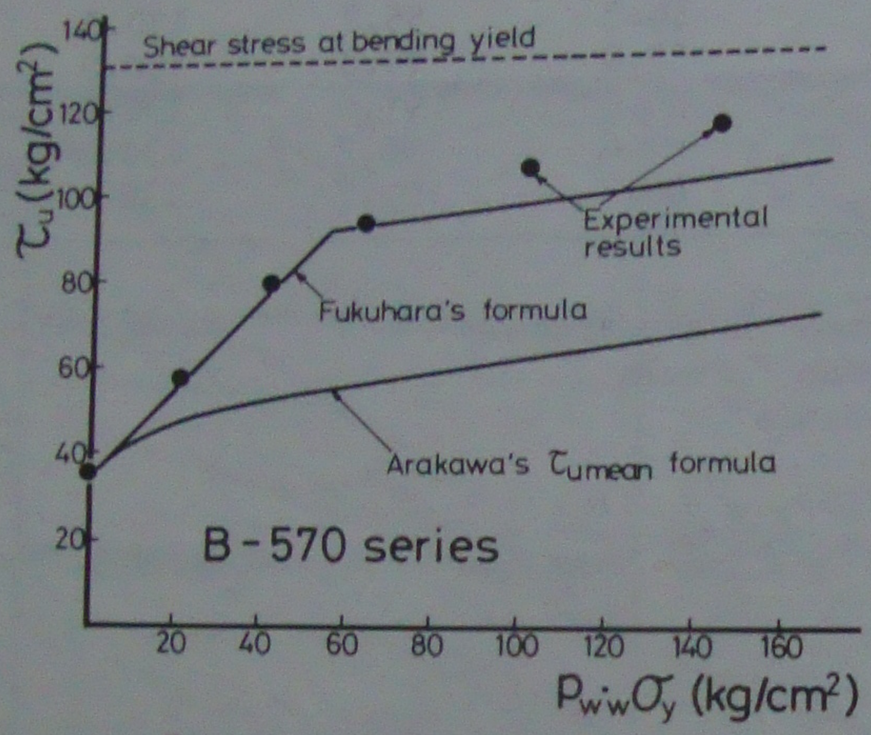

Fig.14 τ_u - $Pw \cdot w\sigma y$ relations of B-570 series

of $Pw \cdot w\sigma y$. Experimental value of the ultimate shear strength is fairly greater than the calculated value applied to Arakawa's τumean formula (Arakawa, 1970). When the experimental value is compared with the calculated value by Fukuhara's formula, both of the value seem to agree well generally. But in B-360 and B-570 series, the rate of the increase of τu in the experiment is greater than that in

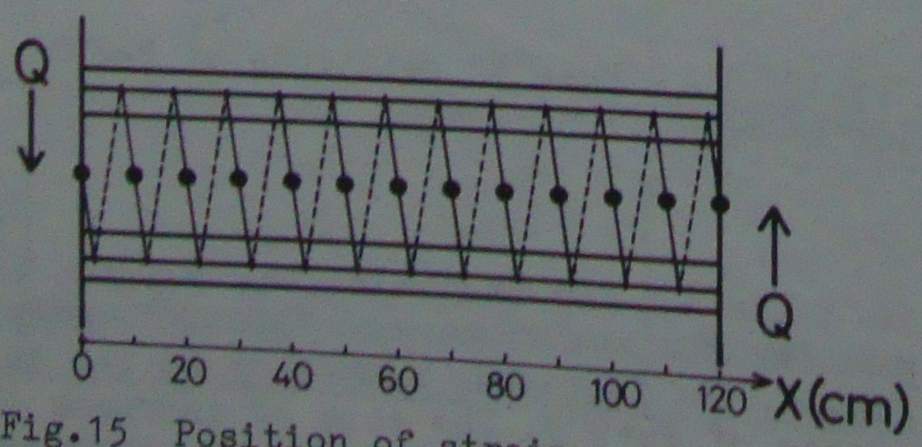

Fig.15 Position of strain gage on shear reinforcement

Fukuhara's formula, according to the increase of $Pw \cdot w\sigma y$. Fukuhara's formula is estimated to be sufficient in practical use, because it gives slightly safety side value in case of beams with high strength concrete.

3.4 Strain distribution of shear reinforcement

Figure 16 through Fig.18 show the strain distribution of shear reinforcement at the ultimate shear strength. The position of strain gages are shown in Fig.15. As the shear reinforcement used in this experiment had helical grooves for bond with concrete except for 4.1mmϕ, the strain gages were put on along the grooves obliquely. Table 5 shows the results of the tension test of reinforcement on which strain gages were put in the same way as specimens. Fig.19 shows a example of their stress-strain curves. $s\varepsilon y'$ was obtained by deviding the yield strength ($w\sigma y$) shown in Table 3 by elastic modulus in this tension test (sE'). Then, the yielding of shear reinforcement in the experiment was judged from this yield strain ($s\varepsilon y'$).

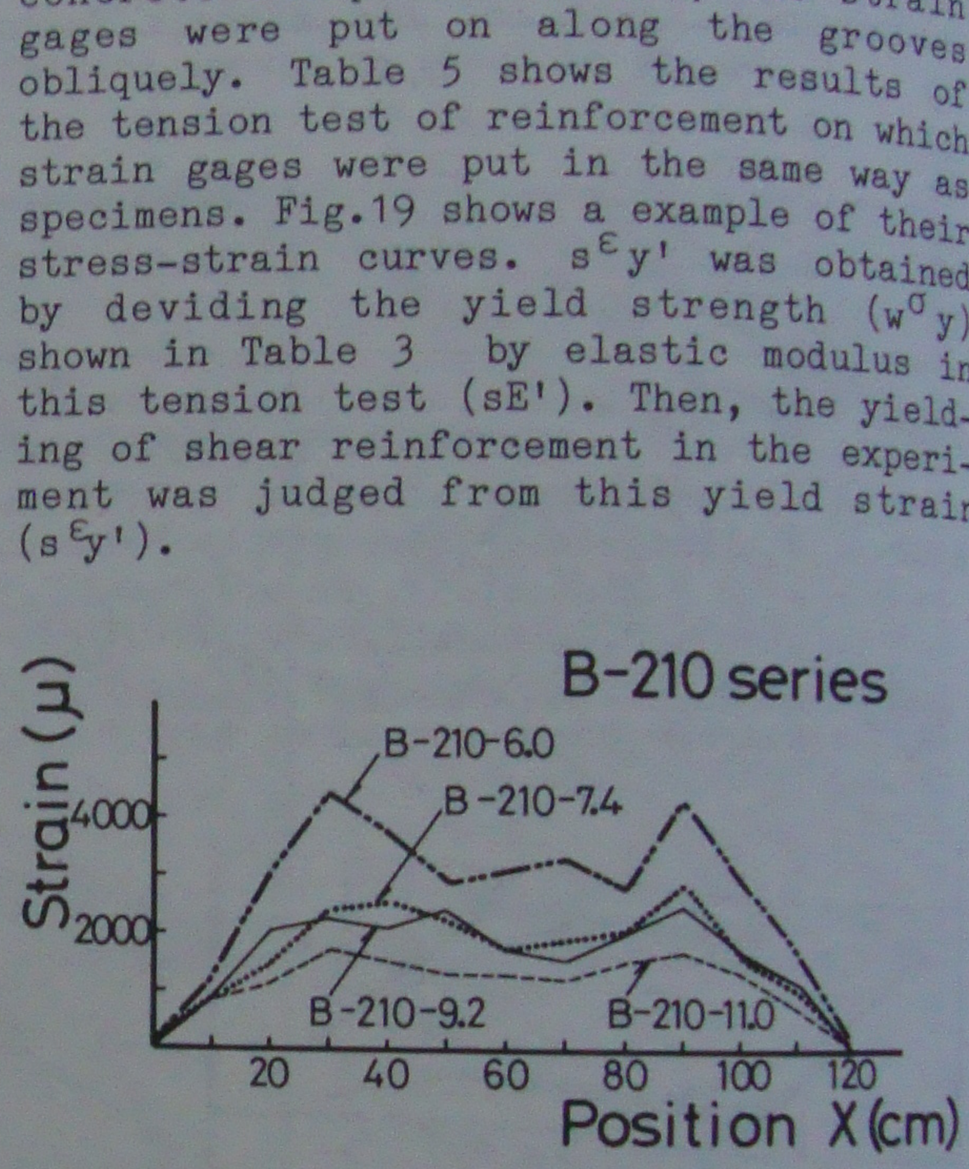

Fig.16 Strain distribution of shear reinforcement of B-210 series

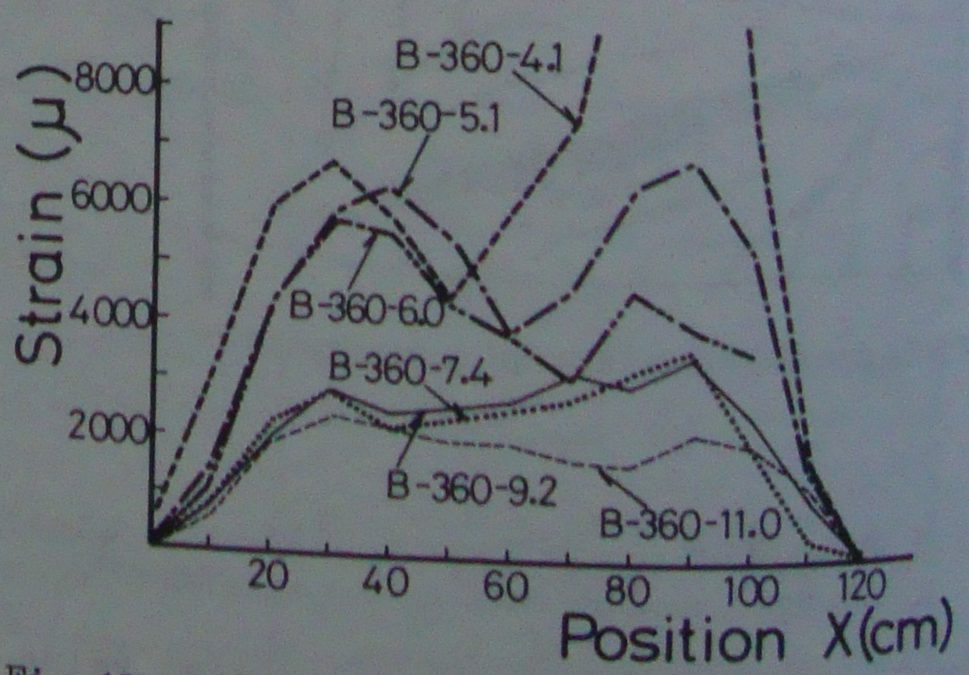

Fig.17 Strain distribution of shear reinforcement of B-360 series

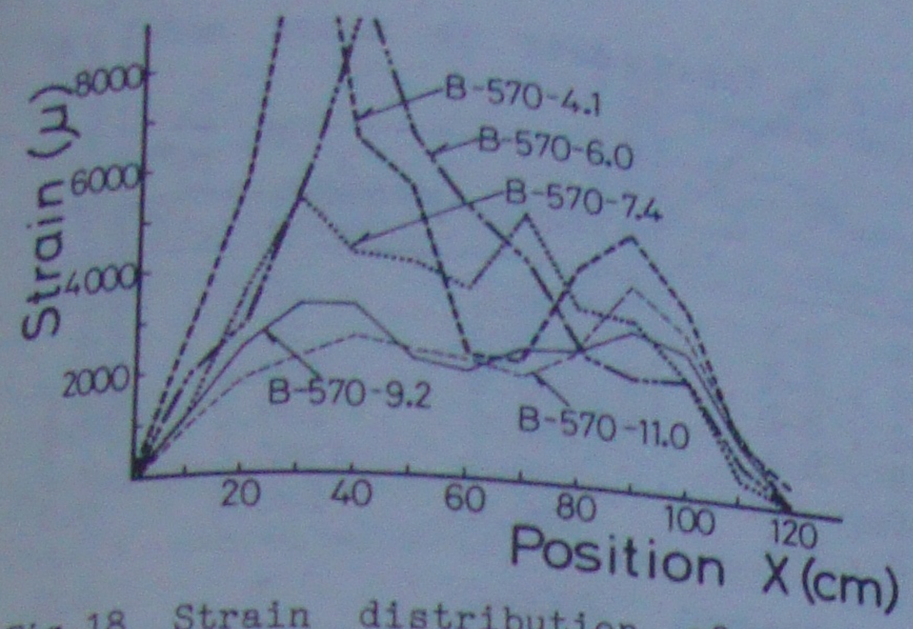

Fig.18 Strain distribution of shear reinforcement of B-570 series

Table 5. Tension test results of shear reinforcement

Steel bar	$_w\sigma_y^*$ (kg/cm^2)	$_sE'$ ($\times 10^6$kg/cm^2)	$_s\varepsilon_y'$ ($\times 10^{-6}$)
4.1	14200	2.09	6800
5.1	14500	2.13	6800
6.0	13600	2.39	5700
7.4	14500	2.54	5700
9.2	14300	2.38	6000
11.0	14600	2.56	5700

* 0.2% proof stress

As for B-210 series, the yielding of shear reinforcements was not observed in all specimens. As for B-360 series, the yielding of shear reinforcements was observed in B-360-4.1, B-360-5.1 and B-360-6.0, but not observed in B-360-7.4, B-360-9.2 and B-360-11.0 with large $Pw \cdot {}_w\sigma_y$. As for B-570 series, yielding of shear reinforcement was observed in B-570-4.1 and B-570-6.0, but not observed in B-570-9.2 and B-570-11.0. In B-570-7.4, the shear reinforcement was just before yielding.

That is, in the range of small $Pw \cdot {}_w\sigma_y$, the full strength of high tension shear reinforcement was displayed at the ultimate shear strength and in the range of large $Pw \cdot {}_w\sigma_y$ over some value, the shear compression failure of concrete goes ahead without full working of high tension shear reinforcement. In this experiment, it was judged that such boundary value of $Pw \cdot {}_w\sigma_y$ was less than 43 kg/cm^2 in B-210 series , about 50 kg/cm^2 in B-360 series and about 60 kg/cm^2 in B-570 series.

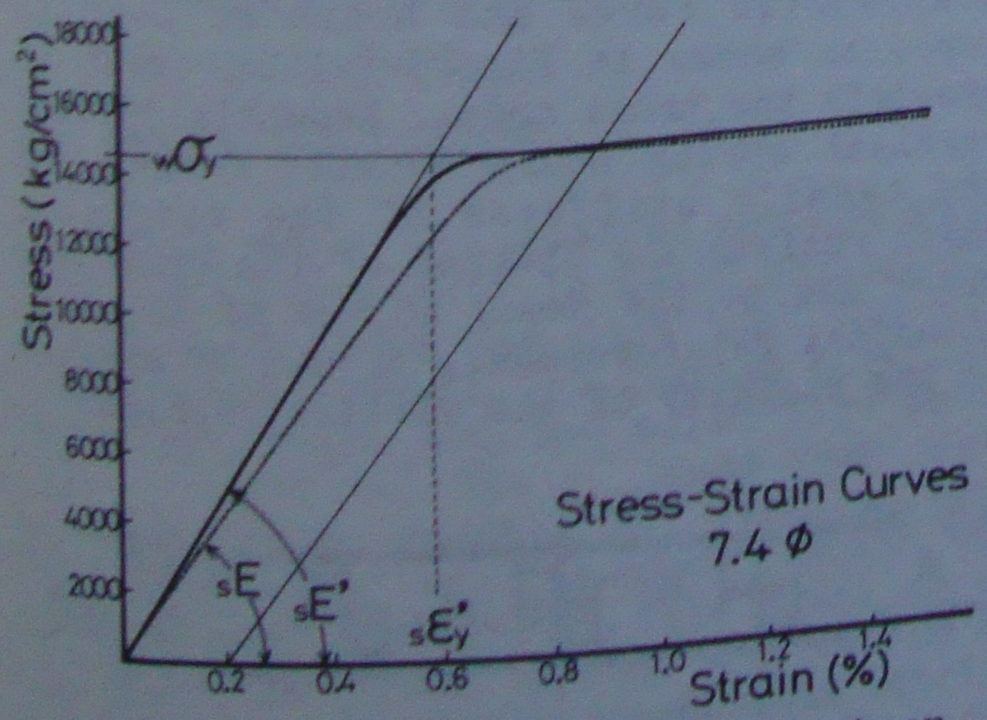

Fig.19 Stress-strain curves of shear reinforcement (ULBON - 7.4φ)

4 CONSIDERATION OF SHEAR TRANSFER MECHANISM

4.1 A simple truss model

A proposed truss model is shown in Fig.20. The concrete truss, which are connected by nodes A, B, C and D, represents a diagonal crack linking the bending compressive zone of beam ends, which develop into the diagonal shear compression failure. The failure of the concrete truss occurs when the strain (or stress) of C-D element reaches a certain value. The truss except for the above mentioned concrete truss construct the beam mechanism. It represents the yielding of longitudinal reinforcement and the yielding of shear reinforcement.

In Fig.16 through Fig.18, the maximum strain of shear reinforcement appears at a distance from the center. It is, however, probably affected by the cracks which cross the position of strain gages or do not. In this struss model, the shear reinforcement in center is made to yield first, to simplify the model and the estimation of the analytical result, but it is considered that this truss model is well worth to explain the tendency of experimental results.

The boundary elements were introduced between the element A-E and A-C, and be-

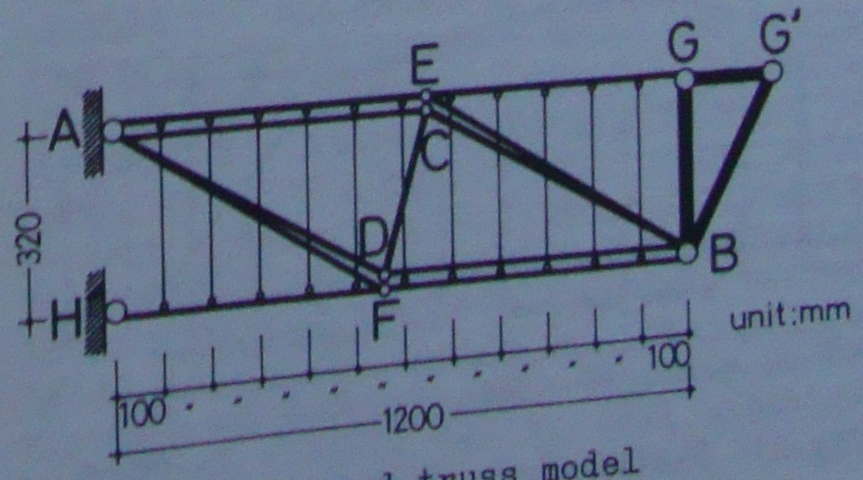

Fig.20 A proposed truss model

tween the element B-F and B-D as shown in Fig.22.

4.2 Determination of rigidity of each elements

The rigidity of each element should be given some general value based on the experimental results or some kind of theory. In this study, however, the values were roughly given from the viewpoint to investigate the possibility to explain the experimental results. They were actually determined as follows.

Elements A-E and B-F: They represent compressive longitudinal reinforcements. The axial rigidity was given the equivalent value considering the reinforcement and the cover concrete. The flexural rigidity was also given that equivalent value, because the splitting crack along the longitudinal reinforcement was supposed to open.

Elements E-G and F-H: They represent tensile longitudinal reinforcement. The axial rigidity should be a slightly larger than that of reinforcement only because of the surrounding concrete. But in this study, that was given the same value as that of elements A-E and B-F. The flexural rigidity was infinitely large, as an extreme value.

Shear reinforcement elements: The axial rigidity was that of only reinforcement, ignoring bond with concrete.

Element C-D: Figure 21 shows the stress distribution caluculated by elastic analysis using Finite Element Method, which is normal to the diagonal linking the bending compressive zone of beam ends. The equivalent length, where the maximum value in the stress distribution uniformly distribute, was about 80 cm. From the analytical results, the area of the cross section of C-D element was determined to be about 1400 cm^2, considering the beam width.

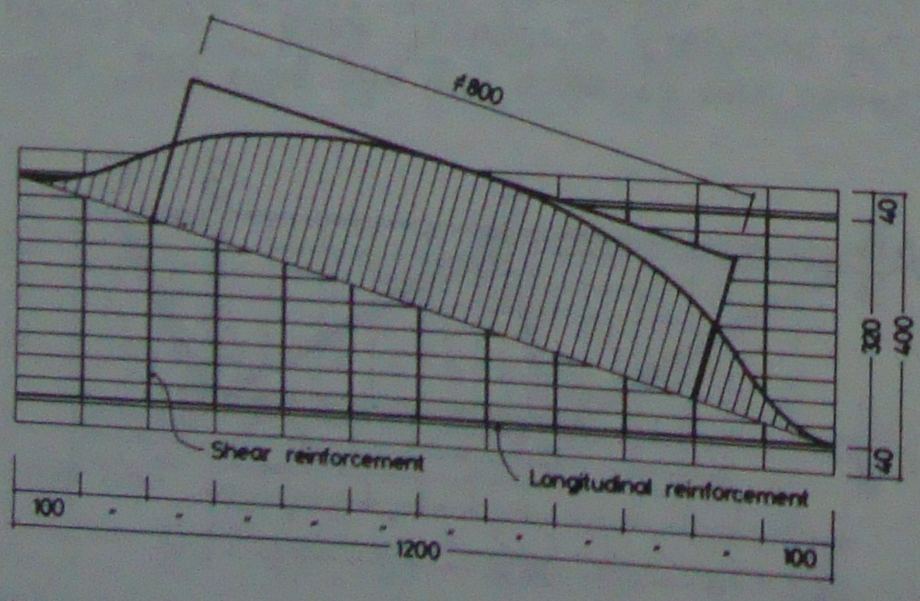

Fig.21 Distribution of tensile stress

Table 6. Input data in truss model of B-360 series

Element	E (ton/cm^2)	A (cm^2)	I (cm^4)
A-E , B-F	2100.0	40.0	300.0
E-G , F-H	2100.0	40.0	∞
A-C , B-D	260.0	200.0	∞
C-B , D-A	260.0	200.0	0.0
C-D	260.0	1400.0	0.0
E-B , F-A	260.0	200.0	0.0
Shear reinforcement	2000.0	*	0.0

* Variable

Elements A-C, A-D, A-F, B-D, B-C and B-E: To begin with, it was roughly assumed that the area of the cross section of all these elements were equal. Next, the initial rigidity between the shear force and the relative displacement of the truss model was computed, when the rigidity of boundary elements was set to be infinity and the splitting crack along the longitudinal reinforcement did not open. The experimental secant modulus at the occurence of the first bending crack in the relation between the shear force and the relative displacement was obtained. Then, the sectional area of these elements was determined to be 200 cm^2 by making equal the rigidity of the truss model and the experimental secant modulus.

Input data for B-360 series are shown in Table 6.

4.3 Properties of boundary elements

The vertical spring shown in Fig.22 looks like Crack-Link in Finite Element Method. In this study, it is assumed that the virtical spring is sufficiently rigid under compressive force and bears no tensile force as shown in Fig.23-(a) in order to symplify the truss model. Essentially, the vertical spring bears tensile force. And the tensile stiffness of the concrete, which resists the opening of the splitting crack due to the dowel action of the longitudinal reinforcement, should be applied to the rigidity of the vertical spring

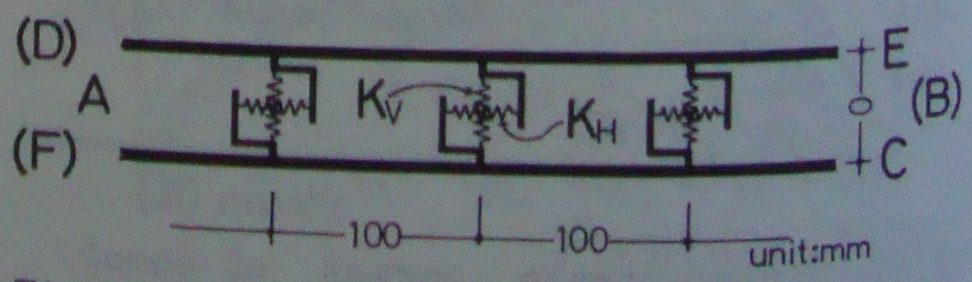

Fig.22 Boundary elements

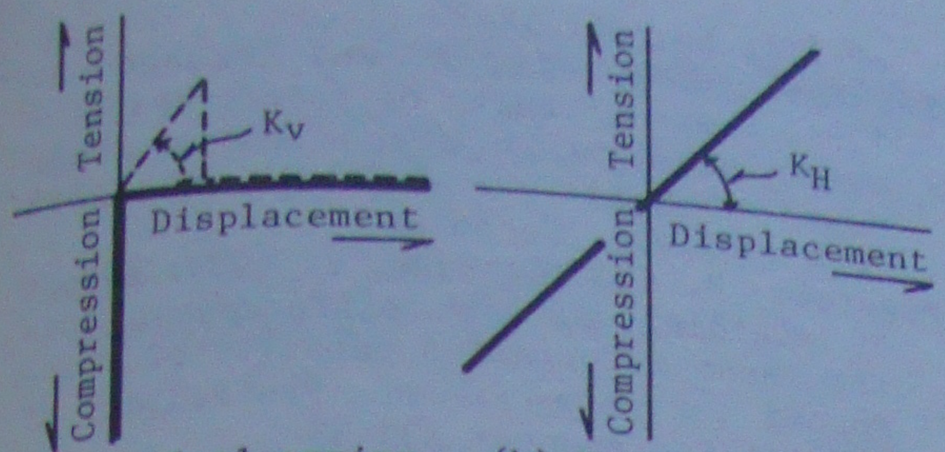

(a) Vertical spring (b) Horizontal spring

Fig.23 Characteristics of boundary element

(Kv) as shown by broken line in Fig.23-(a). In the ultimate state, however, it seems that only the shear reinforcement resists the dowel action of the longitudinal reinforcement after the opening of the splitting crack. That is why the vertical spring bears no tensile force. The elongation of the vertical spring is considered to represent the width of the splitting crack.

The horizontal spring looks like Bond-Link in Finite Element Method. It represents the bond resistance between the longitudinal reinforcement and the concrete, and has the characteristics shown in Fig.23-(b). When the vertical spring elongates and the splitting crack opens, the rigidity of bond resistance (K_H) is made to be zero assuming that the bond resistance is perfectly lost.

4.4 Boundary condition for calculation

Node A and H are supported with pin, joints. Node B and G are jointed with rigid truss elements G-B ,B-G' and G-G'. The equally forced vertical displacement is given the nodes G, G' and B. Then, the anti-symmetric bending moment condition is produced. The horizontal displacement is free, because of no axial force.

4.5 Analytical results

Figure 24 shows the relation between shear force (Q) and $Pw \cdot w\sigma y$ in B-360 series. The broken line shows the case that the concrete truss element C-D reaches a certain value of strain and the solid line shows the case that the shear reinforcement in center reaches its yield stress. For reference, experimental results are pointed with symbol "●". The breaking of the concrete truss element C-D should be judged when its stress reaches the tensile strength of concrete. It will be, however, overestimation to regard the uni-axial

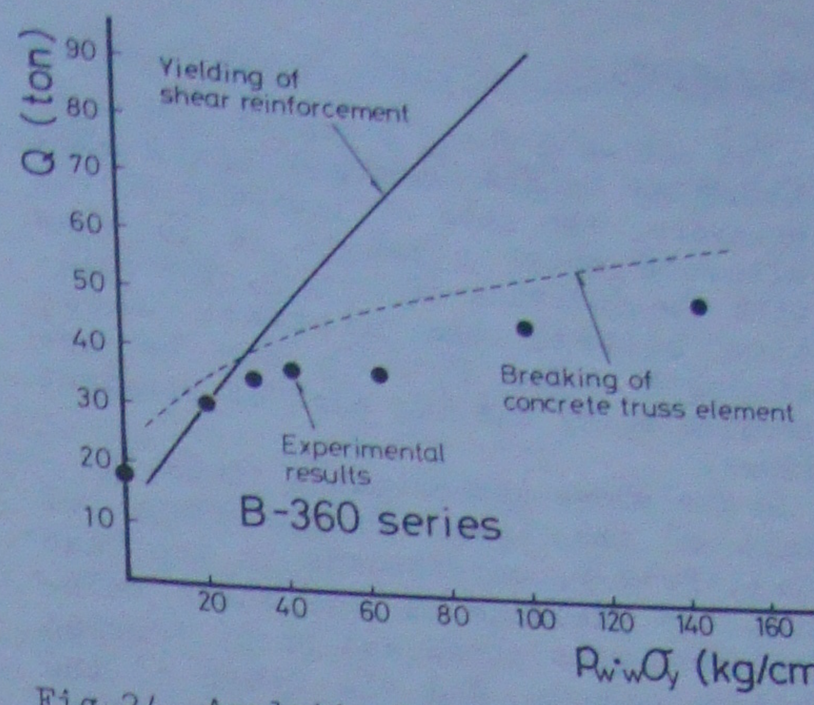

Fig.24 Analytical results by truss model

tensile strength as the criterion for breaking of C-D element. Because at the ultimate state, plural diagonal cracks appear and one of them is dominant to the shear failure. And because the concrete is under bi-axial stress condition at least. Comparing with the experimental results, it was proved that the adoption of about a half of uni-axial tensile strength gave a well agreement between the computed and the experimental results. Then, in Fig.24, a half of uni-axial tensile strength was adopted for the criterion for breaking of C-D element.

In the range of small $Pw \cdot w\sigma y$, the vertical spring of boundary element much elongates. The dowel action of longitudinal reinforcement becomes large and the splitting crack generates. Then, the yielding of shear reinforcement precedes. In the range of large $Pw \cdot w\sigma y$, the elongation of shear reinforcement is small, that is, the elongation of the vertical spring of boundary element is small. Then, element A-E and A-C (also element B-F and B-D) work as one body and the stress of C-D element tends to be large. Then, C-D element breaks before yielding of shear reinforcement. That well agrees with the experimental results in tendency

When the strength of concrete becomes higher, the higher stress level can be adopted for the breaking criterion of the concrete truss elememt C-D. The broken line in Fig.22 moves upward. Therefore, the boundary value of $Pw \cdot w\sigma y$ between the range where the yielding of shear reinforcement goes ahead at shear failure and the range where the shear compression failure of the concrete precedes, becomes large according to the increase of the strength of concrete. The tendency of experimental results can be well explained by this truss model.

5 CONCLUSIONS

(1) The ultimate shear strength increases acording to the increase of $Pw \cdot w\sigma_y$. Howeverr, the rate of increase of the ultimate shear strength is in slow with the increase of $Pw \cdot w\sigma_y$. The relation between the ultimate shear strength and $Pw \cdot w\sigma_y$ can be approximated by the two part of straight lines.

(2) In the above approximated lines, a part of the lines in the range of small $Pw \cdot w\sigma_y$, corresponds to the case that the yielding of the shear reinforcement goes ahead and shear tension failure occurs. And the other of the lines in the range of large $Pw \cdot w\sigma_y$, corresponds to the case that the diagonal shear compression failure of concrete precedes before yielding of shear reinforcement.

(3) The value of $Pw \cdot w\sigma_y$ at the intersection of the above approximated lines, increases according to the increase of the concrete strength.

(4) By using the higher strength concrete the ultimate shear strength is made to increase even if the value of $Pw \cdot w\sigma_y$ is fixed. And the rate of increase of the ultimate shear strength with the the increase of $Pw \cdot w\sigma_y$ becomes large.

(5) The simple truss model was proposed. The tendency of the above experimental results can be well explained by the truss model taking account of the compatibility of deflection as well as the equilibrium of forces in the truss model.

ACKNOWLEDGEMENT

The authors wish to thank Associate Professor Akira WADA of Tokyo Institute of Technology for utilizing the computer program for the analysis which has been developed by him.

REFERENCES

Fukuhara, M., Kokusho, S. and Eigawa, T. 1979. Experimental studies of the ultimate shear strength and deformation capacity in reinforced concrete members with high tension shear reinforcement. Proceedings of AICAP Symposium, Vol.2, Rome: 157-164

Fukuhara, M., Kokusho, S. 1982. Effectiveness of high tension shear reinforcement on reinforced concrete members (Beams subjected to bending moment and shear force). Transaction of AIJ, No.320: 12-20

Fukuhara, M., Wada, A. and Kokusho, S. 1984. Shear strength of reinforced concrete beams with high tension shear reinforcement. Proceedings of IABSE 12th Congress, Vancover

Muguruma, H. and Watanabe, F. 1979. Effect of yielding in web reinforcement upon the shear deformation capacity of reinforced concrete column. Proceedings of JCI 1st Conference: 333-33

Muguruma, H., Watanabe, F., Kohno, K. and Tsujimoto, T. 1980. New simulation test method on shear mechanism and several results on the effect of web reinforcement. Proceedings of JCI 2nd Conference: 469-472

Muguruma, H. and Watanabe, F. 1981. Improving of frexural ductility of reinforced concrete column by the lateral confinement with high yield hoop reinforcement. Proceedings of JCI 3rd Conference: 437-440

NETUREN Co.,Ltd. 1985. Design standard for using high tension steel ULBON as shear reinforcement in reinforced concrete beams and columns

Kobayashi, J., Ito, M. et al. 1983. Test on reinforced concrete columns using high tensile bars for shear reinforcement. Summaries of Technical Papers of Annual Meeting AIJ: 2132-2124

Muguruma,H., Watanabe, F. et al. 1985. Ductility improving of ultra-high strength prestressed spun concrete pile by lateral confining concrete. Proceedings of JCI 7th Conference: 465-468

Yamaguchi, s., Sanda, D., Ishida, J. et al. 1985. Experimental study of high-rised reinforced concrete buildings (Part 1-3). Summaries of Technical Papers of Annual Meeting AIJ, Vol.C: 139-144

Kokusho, s., Wada, A., Kobayashi, K. et al. 1986. Study on the improvement in bearing capacity and deformability of prestressed high strength concrete pile (Part 3-4). Summaries of Technical Papers of Annual Meeting AIJ, Vol.C: 1245-1248

Ito, M., Mogami, T. et al. 1986. Test of structural members in tall buildings utilizing the R.C. layered construction system (Part 1-5). Summaries of Technical Papers of Annual Meeting AIJ, Vol.C: 175-184

Arakawa, T. 1970. Allowable shear stress and shear reinforcing in reinforced concrete beams. Concrete Journal, Vol.8, No.7